Defense Technical Information Center Compilation Part Notice

ADP012599

TITLE: Enhanced Photoluminescence from Long Wavelength InAs Quantum Dots Embedded in a Graded [In,Ga]As Quantum Well

DISTRIBUTION: Approved for public release, distribution unlimited

This paper is part of the following report:

TITLE: Progress in Semiconductor Materials for Optoelectronic Applications Symposium held in Boston, Massachusetts on November 26-29, 2001.

To order the complete compilation report, use: ADA405047

The following component part numbers comprise the compilation report:
ADP012585 thru ADP012685

Mat. Res. Soc. Symp. Proc. Vol. 692 © 2002 Materials Research Society

Enhanced Photoluminescence from Long Wavelength InAs Quantum Dots Embedded in a Graded (In,Ga)As Quantum Well

L. Chen, V. G. Stoleru, D. Pal, D. Pan, and E. Towe
Department of Electrical and Computer Engineering, University of Virginia, Charlottesville, Virginia 22904

ABSTRACT

Three sets of self-organized InAs quantum dots (QDs) embedded in an external InGaAs quantum well samples were grown by solid source molecular beam epitaxy (MBE). By modifying Indium composition profile within quantum well (QW) region, it's found the photoluminescence emission from quantum dots can be greatly enhanced when employing a graded quantum well to surround QDs. This quantum dots in a graded quantum well structure also preserves the long wavelength (1.3 μm) spectrum requirement for the future use in optoelectronics devices.

INTRODUCTION

The first GaAs-based quantum-dot laser was reported in 1994 [1]. Since then, remarkable progress has been made in the development of this device. Edge-emitting lasers operating from 1.0 to 1.3 μm with very low threshold currents have been reported [2,3,9]; in addition, vertical-cavity surface-emitting lasers (VCSELs) have also been successfully demonstrated [4].

There are currently several approaches to grow 1.3 μm (In,Ga)As quantum dots by MBE. These include (i) the alternate supply of group-III and group-V source materials to form the (In,Ga)As dots [5], (ii) very slow growth (<0.01 ML/sec) of the InAs dots at high substrate temperatures [6], (iii) burying the InAs dots with an InGaAs overlayer to reduce the strain [7], and (iv) embedding the InAs dots inside an InGaAs quantum well [8].

Most quantum-dot lasers operating at 1.3 μm appear to have two major unresolved problems: a low density of dots and a weak carrier confinement to the active region. Both of these problems imply low optical gain. In fact, the low gain is believed to prohibit the lasers from operating at the ground state without high-reflectivity coatings [3,10]. One approach to achieving tight carrier confinement is to use growth method (iv), which embeds the dots in an InGaAs quantum well. In addition to serving as a strain reducing (and hence a wavelength tuning) layer, the InGaAs quantum well also serves to confine carriers within the vicinity of the quantum-dot layer, thus promoting capture within the dots [9].

In this paper, we report a modified structure with InAs quantum dots embedded in a graded InGaAs quantum well, which not only tunes the QDs emission to 1.3 μm, but also greatly enhances the photoluminescence (PL) efficiency.

EXPERIMENT

The samples in our study were grown in a Riber 32P solid source MBE system on semi-insulating (001) GaAs substrates. The basic structure for PL study consists of a 250 nm GaAs buffer grown at a substrate temperature of 580°C, a 90 nm GaAs layer with a reduced substrate temperature at 490°C, 1~2.5 ML InAs quantum dots symmetrically sandwiched in an 8 nm

$In_xGa_{1-x}As$ layer and a final 90 nm GaAs top layer. For Atomic-Force Microscopy (AFM), samples with similar structures, but with growth stopped after InAs deposition, were grown. The growth rate of the InAs dots was 0.05 ML/sec. The substrate holder was continuously rotated to improve the uniformity. A Coherent Argon ion laser (λ=488 nm) is used for PL and the emitted radiation was detected by a SPEX 500M spectrometer with a cooled Hamamatsu Ge detector. A Bomen MB155S FTIR is used for photocurrent (PC) measurement and a PSI AutoProbe CP is used for AFM.

RESULTS AND DISCUSSIOIN

Fig. 1 shows the PL spectra of InAs QDs embedded in an 8 nm $In_xGa_{1-x}As$ QW with different Indium composition x under different InAs deposition. From Fig.1, it's seen that the wavelength can be red shifted with the increase of InAs deposition. When InAs content is increased to 2.5 ML, the peak wavelength of QDs in an $In_{0.18}Ga_{0.82}As$ QW reaches 1.3 μm but with apparent decrease of PL intensity, which indicates the possible formation of defects in this highly strained structure. Our best result is from 2.5 ML InAs QDs in an $In_{0.15}Ga_{0.85}As$ QW.

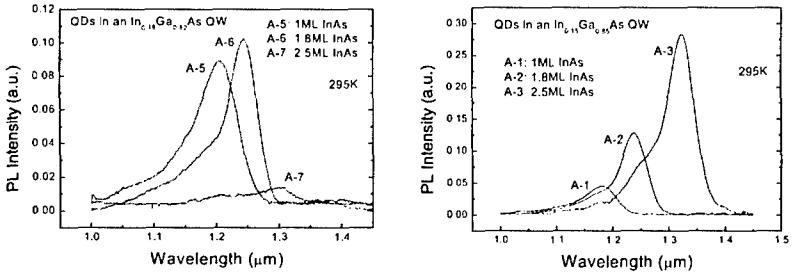

Fig. 1. Room temperature photoluminescence spectra of InAs quantum dots embedded in an 8 nm $In_xGa_{1-x}As$ quantum well with various InAs deposition.

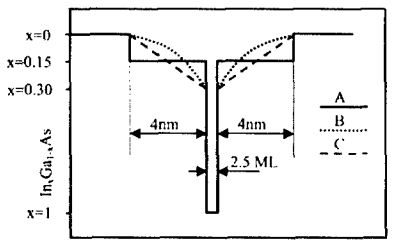

Fig. 2. Schematic structure of three different sets of quantum dot samples.

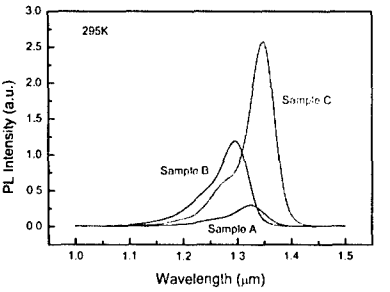

Fig. 3. Room-temperature PL spectra of QD samples at an optical excitation level of ~30 W/cm^2.

To further study the influence of Indium composition profile in the $In_xGa_{1-x}As$ QW, We modify the QW growth. A schematic of the generic structures is shown in Fig. 2. Structure A consists of 2.5 monolayers of InAs QDs sandwiched at the center of an 8 nm $In_{0.15}Ga_{0.85}As$ layer. Structure B consists of 2.5 monolayers of InAs QDs sandwiched at the center of an 8 nm In_xGa_{1-}

$_x$As layer; where the bottom half of the $In_xGa_{1-x}As$ layer is graded from x = 0.03 to x = 0.3 and the top half is graded from x = 0.3 to x = 0.03. The change of Indium composition in the graded QW was achieved by gradually increasing or decreasing the Indium cell's temperature, which resulted in a curved shape of Indium distribution. The structure C is similar to structure B except that InAs/GaAs superlattice layers are used to form a quasi-linear indium distribution along the growth direction.

Room temperature photoluminescence spectra of three typical samples A, B, and C are shown in Fig. 3. The emission from the ground state transition for all three samples is at, or beyond 1.3 μm, with sample C extending to 1.35 μm. The spectral linewidths at half-maximum intensity for these three samples are Δ = 48 meV, Δ = 53 meV, and Δ = 39 meV, which shows the inhomogeneous broadening in all the samples. The grading of the $In_xGa_{1-x}As$ QW does not have apparent effect on the uniformity of the dots. What the grading appears to do is to improve the efficiency of emission. The peak intensity of sample C, for example, is about 8.7 times higher than that of sample A. Since the only difference in the three samples is the structure of the $In_xGa_{1-x}As$ layer into which the quantum dots are embedded, it is reasonable to speculate that the enhancement of PL intensity is due to the grading. There may be two possible reasons that account for this enhancement. One is that, in a graded QW, the energy band is also graded; this helps to drive the carriers into the quantum well, and hence into the quantum dots. Because of the three-dimensional nature of quantum dots, the graded potential also exists in the lateral direction; this enhances spatially carrier capture within the dots. The second reason for the enhancement is the smoothing effect of the InAs/GaAs superlattice. The use of superlattice causes smooth transition of the lattice parameter from the GaAs to the InAs, thus may help to reduce the defects formation. The defects, if present, would form loss channels in the electron-hole recombination process.

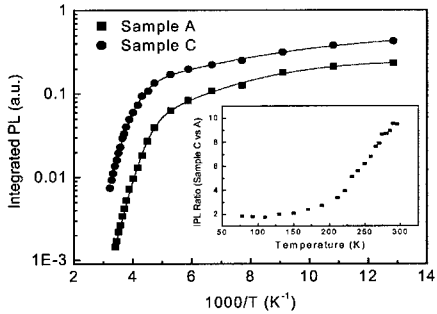

A: E_1=289 meV, E_2=41 meV
C: E_1=255 meV, E_2=25 meV

$$I(T)=\frac{I_0}{1+C_1\exp(-E_1/kT)+C_2\exp(-E_2/kT)}$$

Fig. 4. The Arrhenius plots of the IPL intensity of sample A and C at an excitation level of ~10 W/cm^2. The solid lines are fitted by the equation shown on the figure. The inset is the ratio of the IPL intensity of sample C to that of sample A as a function of temperature.

We have further studied the temperature-dependent integrated photoluminescence (IPL) intensity of samples A and C. The Arrhenius plots for these two samples are shown in Fig. 4. As seen from the figure, photoluminescence enhancement of sample C is more dramatic at higher temperatures (see the inset in Fig. 4). We fit the variation of the IPL intensity data with temperature by a generic empirical relationship [11] shown on the figure, where E_1 and E_2 are the thermal activation energies for loss mechanisms active at certain temperature ranges, k is the

Boltzmann constant, T is the temperature, and C_1, C_2 and I_0 are fitting constants. In a physical model, these constants would take into account the recombination rates and the geometric dimensions of the dots. In Fig. 4, the solid lines are the fitting curves; the filled circles and squares represent experimental data. The extracted thermal activation energies are E_1=289 meV, and E_2=41 meV for sample A; and E_1=255 meV and E_2=25 meV for sample C. A calculation (which we will discuss later) shows that the energy difference between the ground state in the conduction band of a dot and the band-edge of the surrounding (In,Ga)As quantum well at 300 K is about 317 meV for structure A and 267 meV for sample C. These energy differences are quite close to the measured activation energies E_1 (which dominates the quenching at high temperature) for sample A and C. Note that the IPL intensity has a quenching threshold temperature ~190 K for sample C, and ~170 K for sample A. Either a fast trapping of carriers to the QDs or a reduced loss channel around QW can result in a higher quenching threshold. Our results here are similar to those of Ru *et al.* who used hydrogen passivation (in order to reduce the defect concentrations in their samples) to enhance the photoluminescence emission [12].

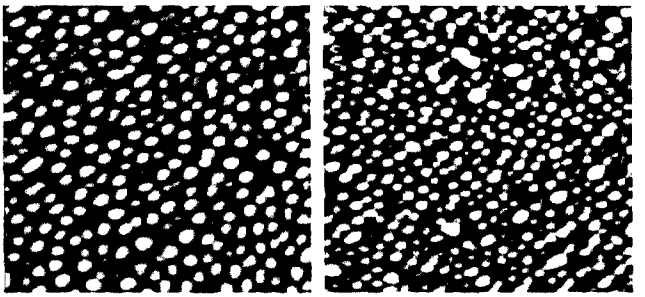

Fig.5. AFM photo-micrographs of the morphology of structure A and C.

We have also examined the possible effects of the grading on the dot density and uniformity. Two structures similar to sample A and C were grown for AFM observation. Figure 5 shows that there are no major differences in the two samples. Sample A, for example, has a dot density of around 2.5×10^{10} cm^{-2}, while sample C has a dot density about 2.8×10^{10} cm^{-2}. The true size of the dots cannot be determined from AFM measurement; reasonable estimates, however, can be obtained from cross-sectional TEM studies.

To show that the graded quantum well structure does not substantially modify the basic band structures, we have studied both the intensity dependent photoluminescence and photocurrent at LN_2 (78 K) temperature. In Fig. 6, we show the PL emission from sample A and sample C at high pump levels, and in Fig. 7, we show the photocurrent spectra of sample A and C excited by a broad band incident light (filtered by GaAs). There are clearly four transition energy peaks for each sample; the peaks occur at almost identical locations for both samples. To confirm these transition levels are from QDs, we have carried out some analytical calculations to determine the interband transition energies. These calculations require information on the strain distribution inside and around the dots. The strain generally depends on the shape and size of the dots, which

are difficult to determine accurately in most experimental situations. For our dots, we estimate their lateral base to be around 15 nm; the base to height ratio for sample A is about 7; and it is

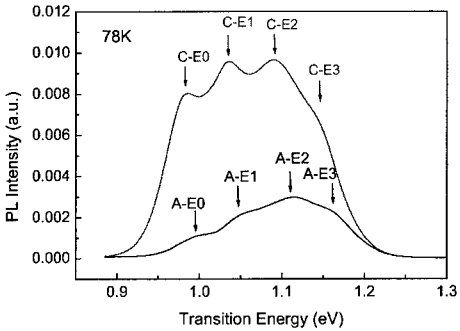

Fig. 6. Low-temperature (78 K) PL spectra of sample A and C at high optical pumping level.

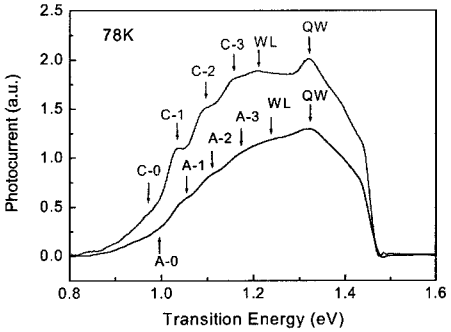

Fig. 7. Low-temperature (78 K) Photocurrent spectra of sample A and C.

5 for sample C. These estimates are based on our earlier work on buried InAs/GaAs and InGaAs/GaAs quantum dots [13], and on TEM and SEM observations. The estimate on height is further corroborated with *in-situ* RHEED observations where the thickness of an overlayer needed to completely bury an array of dots can give a rough measure of the dot height. For the calculations, we have further assumed that the dots are truncated pyramids.

Structure	Data Source	Transition Energy (eV)				
		Low Temperature (77K)				RT
		E0	E1	E2	E3	E0
A	Experimental	1.019	1.056	1.102	1.154	0.934
	Calculated	1.0162	1.0572	1.0951	1.1500	0.9405
C	Experimental	0.987	1.036	1.083	1.139	0.919
	Calculated	0.9830	1.0379	1.0809	1.1315	0.9138

Table I. Experimental and calculated transition Energies for sample A and C

The electronic spectra here are calculated in the envelope function approximation using an eight-band, strain-dependent Hamiltonian based on the **k·p** method [14]. The method takes into account the coupling among the light- and heavy-hole bands, and the split-off valence bands. It also includes the linear coupling between the conduction and valence bands. The lack of inversion symmetry in the zinc-blende structure, however, is neglected. The effect of strain is included via deformation potential theory [15], and the Luttinger-Kohn parameters are calculated according to the method by Pollak [16], and Bir and Pikus [17]. Because the quantum dots are in the strong confinement regime, additional binding energy from the Coulomb interaction is neglected. The bound states of QDs are found by numerically solving the Schrödinger equation, by invoking periodic boundary conditions, expanding the wavefunctions in terms of normalized

plane-wave states, and diagonalizing the obtained matrix. The calculated transition energies for sample A and C are shown in Table I. We have also shown the experimentally determined values from the photoluminescence data by multi-peaks Gaussian fitting. The experimental and the calculated transition energies are in reasonably good agreement.

CONCLUSIONS AND ACKNOWLEDGEMENT

In summary, we have shown that the photoluminescence efficiency of InAs quantum dots can be enhanced by embedding them in a graded (In,Ga)As quantum well structures. Furthermore, our proposed approach has the virtue of promoting carrier capture in potential laser structures in addition to allowing emission at the desirable telecommunications wavelength of 1.3 μm.

This work is supported under grant number DAAD19-00-1-0442 of the US Army Research Office, Research Triangle Park, North Carolina, and by the US Army Research Laboratory, Adelphi, Maryland.

REFENENCES

[1] N. Kirkstaedter, N. Ledentsov, M. Grundmann, D. Bimberg, V. Ustinov, S. Ruvimov, M. Maximov, P. Kop'ev, and Zh. Alferov, Electron. Lett. **30**, 1416 (1994).
[2] G. Park, O.B. Shchekin, D.L. Huffaker, and D.G. Deppe, IEEE Photon. Tech. Lett. **12**, 230 (2000).
[3] D.L. Huffaker, G. Park, Z. Zou, O.B. Shchekin, and D.G. Deppe, Appl. Phys. Lett. **73**, 2564 (1998).
[4] J.A. Lott, N. Ledentsov, V. Ustinov, N. A. Maleev, A. E. Zhukov, A. R. Kovsh, M. V. Maximov, B. V. Volovik, Zh. I. Alferov, and D. Bimberg, Electron. Lett. **36**, 1384 (2000).
[5] D.L. Huffaker and D.G. Deppe, Appl. Phys. Lett. **73**, 520 (1998).
[6] R. Murray, D. Childs, S. Malik, P. Siverns, C. Roberts, J.M. Hartmann, and P. Stavrinou, Jpn. J. Appl. Phys. 38, 528 (1999).
[7] K. Nishi, H. Saito, and S. Sugou, Appl. Phys. Lett. **74**, 1111 (1999).
[8] A. Stintz, G. T. Liu, H. Li, L. F. Lester, and K. J. Malloy, IEEE Photon. Tech. Lett. **12**, 591 (2000).
[9] G. T. Liu, A. Stintz, H. Li, T.C. Newell, A.L. Gray, P.M. Varangis, K. J. Malloy, and L. F. Lester, IEEE Journal of Quan. Electron. **36**, 1273 (2000).
[10] N. Hatori, M. Sugawara, K. Mukai, Y. Nakata, and H. Ishikawa, Appl. Phys. Lett. **77**, 773 (2000).
[11] Y. Wu, K. Arai, and T. Yao, Phys. Rev. B **53**, 10485 (1996).
[12] E. C. Le Ru, P. D. Siverns, and R. Murray, Appl. Phys. Lett. **77**, 2446 (2000).
[13] V. G. Stoleru, D. Pal, and E. Towe, *Mater. Res. Soc. Proc.* Vol. **642**, J.1.7.1-6, Boston, MA (2000).
[14] T.B. Bahder, Phys. Rev. B **41**, 11992 (1992).
[15] O. Stier, M. Grundmann, and D. Bimberg, Phys. Rev. B **59**, 5688 (1999).
[16] F. H. Pollak, *Semiconductors and Semimetals*, Academic Press, Inc., New York, Volume **32**, pp. 17 (1990).
[17] G. E. Pikus and G. L. Bir, Sov. Phys. Solid State **1**, 1502 (1960).